Monthly Notices
of the
ROYAL ASTRONOMICAL SOCIETY

Mon. Not. R. Astron. Soc. **405,** 2132–2140 (2010) doi:10.1111/j.1365-2966.2010.16655.x

Co-orbital satellites of Saturn: congenital formation

A. Izidoro,[1⋆] O. C. Winter[1⋆] and M. Tsuchida[2⋆]

[1] *UNESP, Univ Estadual Paulista – Grupo de Dinâmica Orbital & Planetologia, Guaratinguetá CEP 12.516-410, Brazil*
[2] *UNESP, Univ Estadual Paulista – DCCE-IBILCE, São José do Rio Preto CEP 15.054-000, Brazil*

Accepted 2010 March 1. Received 2010 March 1; in original form 2009 June 27

ABSTRACT

Saturn is the only known planet to have co-orbital satellite systems. In the present work we studied the process of mass accretion as a possible mechanism for co-orbital satellites formation. The system considered is composed of Saturn, a protosatellite and a cloud of planetesimals distributed in the co-orbital region around a triangular Lagrangian point. The adopted relative mass for the protosatellite was 10^{-6} of Saturn's mass and for each planetesimal of the cloud three cases of relative mass were considered, 10^{-14}, 10^{-13} and 10^{-12} masses of Saturn. In the simulations each cloud of planetesimal was composed of 10^3, 5×10^3 or 10^4 planetesimals. The results of the simulations show the formation of co-orbital satellites with relative masses of the same order of those found in the Saturnian system (10^{-13}–10^{-9}). Most of them present horseshoe-type orbits, but a significant part is in tadpole orbit around L_4 or L_5. Therefore, the results indicate that this is a plausible mechanism for the formation of co-orbital satellites.

Key words: planets and satellites: formation – planets and satellites: individual: Saturn.

1 INTRODUCTION

Co-orbital systems are those in which at least two bodies share the same mean orbit. Co-orbital objects that librate around the Lagrangian points L_4 or L_5 are said to be in tadpole orbits, while those that librate around L_4, L_3 and L_5 are said to be in horseshoe-type orbits. Although Lagrange have described the motion of bodies around these equilibrium points in 1788, when he published his *Analytical Mechanics*, only in 1906 a body showing this kind of motion was discovered by Max Wolf in Heidelberg. He found an asteroid librating around the point L_4 of Jupiter in the system Sun–Jupiter. This asteroid is (588) Achiles and at the moment there are more than 3200 know asteroids co-orbiting with Jupiter (http://www.cfa.harvard.edu/iau/lists/JupiterTrojans.html). Apart from Jupiter there are other planets with co-orbital bodies. In 1991 the asteroid 5261 Eureka was discovered librating around the L_5 of Mars (Innanen 1991). Later three more asteroids were discovered: 1998 VF_{31} (Tabachnik & Evans 1999), 1999 UJ_7 (Connors et al. 2005) and 2007 NS_2 (http://www.cfa.harvard.edu/iau/lists/MarsTrojans.html). Neptune has six co-orbital asteroids. All of them librating around its Lagrangian point L_4 (Zhou, Dvorak & Sun 2009).

On the other hand, all the co-orbital satellite systems known are around the planet Saturn (Table 1). The satellite Thetys has two co-orbital satellites. Telesto around its L_4 point and Calypso around its L_5 point. They were discovered in 1980 by observations made from Earth (Reitsema 1981; Veillet 1981). The satellite Dione also has two co-orbital satellites. Helene around its L_4 point and Polydeuces around its L_5 point. Helene was discovered in 1980 by observations made from Earth (Lecacheux et al. 1980; Reitsema, Smith & Larson 1980), and Polydeuces was discovered through images from the Cassini spacecraft (Murray et al. 2005; Porco et al. 2005). In 1981, images from Voyager not only confirmed the existence of the co-orbital system Janus and Epimetheus but also determined their masses and orbital elements. In a suitable rotating coordinate system, both satellites perform horseshoe orbits and reach a distance of only 15 000 km from each other (Yoder et al. 1983).

The satellites Thetys and Dione are of the same size and have mass of the order of 10^{-6} Saturn's mass (Table 2). They also have another interesting common feature. They are in mean motion resonance with a smaller interior satellite. Mimas–Thetys are in 4:2 inclination-type resonance while Enceladus–Dione in a 2:1 eccentricity-type resonance. However, Mimas and Enceladus do not have any co-orbital satellite known until now. A possible explanation for that was given by Mourão et al. (2006) and Christou, Namouni & Morais (2007). Mourão et al. (2006) studied the stability of hypothetical satellites co-orbital to the satellites Mimas and Enceladus. Their results showed that these co-orbital satellites are in stable orbits. Then, they explored the stability of these hypothetical co-orbital satellites putting Mimas and Enceladus at different values of semimajor axis, which they could have occupied in the past, along their orbital migration due to tidal their effects. They found that the hypothetical co-orbital satellites would always be in stable orbits. The only exceptions occurred when Mimas and Enceladus were placed at semimajor axis where they were in mean motion

⋆E-mail: izidoro.costa@gmail.com (AI); ocwinter@pq.cnpq.br (OCW); tsuchida@ibilce.unesp.br (MT)

Table 1. Co-orbital satellites of Saturn (Giorgini et al. 1996; Jacobson 2004; Murray et al. 2005; Porco et al. 2005).

Satellite	Relative mass[a]	Orbit	Density (g cm^{-3})	Radius (km)	$\Delta\theta^b$
Polydeuces	$1\sim 5\times10^{-13}$	L_5 Dione	–	3.25	25.8
Helene	4.48×10^{-11}	L_4 Dione	1.5	16 ± 4	14.8
Telesto	1.25×10^{-11}	L_4 Thetys	1.0	12 ± 3	1.3
Calypso	6.32×10^{-12}	L_5 Thetys	1.0	9.5 ± 1.5	3.6
Janus	3.38e-09	Horseshoe	0.65	$99.3\times95.6\times75.6$	
Epimetheus	9.67e-10	Horseshoe	0.63	$69\times55\times55$	

[a]Mass with respect to Saturn.
[b]Libration amplitude.

Table 2. Satellites of Saturn which have co-orbital satellites in tadpole orbits (Giorgini et al. 1996).

Satellites			
Satellite	Relative mass[a]	Density (g cm^{-3})	Radius (km)
Dione	1.92×10^{-06}	1.469	562.5
Thetys	1.08×10^{-06}	0.956	536.3

[a]Mass with respect to Saturn.

first-order resonance with each other. The hypothetical co-orbital satellites left their tadpole orbits when Mimas and Enceladus were in 4:5, 5:6 or 6:7 mean motion resonances. Therefore, if there were co-orbital satellites of Mimas or Enceladus, they may have lost them along their orbital migration, when passing through specific mean motion resonances.

Dermott & Murray (1981a,b) presented a theory on the tadpole and horseshoe-type orbits for the case of circular and elliptic restricted three-body problem. They also described the co-orbital motion of Janus and Epimetheus through a numerical study combined with perturbation theory. The study was made for a third body of negligible mass. Then, they generalized some of these results for the case when the third body disturbs the other two bodies of the system. One of the main results found was a relation between the co-orbital trajectory and its associated zero velocity curve.

There are several studies on the origin of the Trojan asteroids, but not too many on the origin of the co-orbital satellites. The origin of these satellites and Trojans asteroids are believed to be associated to one of the following mechanisms (Smith et al. 1981; Yoder et al. 1983): (i) capture by gas drag, (ii) congenital formation or (iii) rupture of a parent body.

Chanut, Winter & Tsuchida (2008) studied the mechanism of capture by drag. They considered several values for the relative mass of the secondary body, from 10^{-7} to 10^{-3}. They explored the orbital evolution of planetesimals under orbital decay toward the secondary body orbit. There are three possible outcomes along such evolution: collision with the secondary body, capture in the co-orbital region or crossing the co-orbital region toward the central body. Once a planetesimal is captured in a co-orbital trajectory, its amplitude of oscillation around one of the triangular Lagrangian points shrinks until it is fixed over the Lagrangian point. They also showed that the location of the Lagrangian points change according to the density of the gas.

With the numerous discoveries of the extrasolar planets, Beaugé et al. (2007) analysed the formation of hypothetical Earth-type co-orbital planets in extrasolar systems. The central body was taken as equal to $1\,M_\odot$ and the giant planet with Jupiter's mass. They considered two scenarios of formation, one gas-free scenario and another rich-gas scenario. In both of them there were the formation of a single co-orbital of the terrestrial type, but due to gravitational instability with other bodies, the accretion process was not efficient.

In this paper we study the mechanism of congenital formation of co-orbital satellites and in some points this mechanism is similar to the one adopted in Beaugé et al. (2007). According to the modern theories of planetary formation, in the beginning of the Solar system formation there was a cloud of gas and dust that settled in a disc. Because of several factors the gas dissipated along the time. In the first stages the particles were of the size of submicrometres up to the order of centimetres. This disc of gas and dust gradually generated larger bodies through physical collisions leading to agglomeration. Successive encounters among them resulted in a large number of metre-sized aggregates. From these objects originated planetesimals of the order of kilometres. Further encounters between planetesimals led to the formation of the planet's progenitors of terrestrial size or even 10 times this size (Armitage 2007). The formation of planetary satellite systems is thought to have followed a very similar way (Safronov 1969; Wetherill 1980, 1990; Hayashi, Nakazawa & Nakagawa 1985; Greenberg 1989).

In the present work we consider an intermediate stage of Saturn's satellite system formation. In this stage all the major satellites are almost formed (here called protosatellites), there is almost no gas left, but there is still plenty of small planetesimals in the disc. Our model of study is characterized by a central body (Saturn), a secondary body (protosatellite) and a cloud of plantesimals. Since it is assumed that the protosatellite has already a significative mass, which is several orders of magnitude larger than the planetesimals, it defines (together with the planet) the structure of the phase space with the five Lagrangian points. Then, we consider a cloud of planetesimals in the co-orbital region around one of the triangular Lagrangian points, under the gravitational influence of Saturn and the protosatellite. The collision between planetesimals is considered constructive and through this accretion process larger bodies are built in the co-orbital region.

This paper has the following structure. In the next section we present the methodology and assumptions adopted in our numerical simulations. The results of the simulations are presented in Section 3. Finally, in the last section we present some final comments and our conclusions.

2 METHODOLOGY

The dynamical system considered is composed of Saturn (the central body), a protosatellite and a cloud of planetesimals. The mass of the protosatellite was chosen to be 10^{-6} of Saturn's mass, which is close to the masses of Dione and Thetys (Table 2). It is placed in a circular orbit with the semimajor axis equal to that of Thetys.

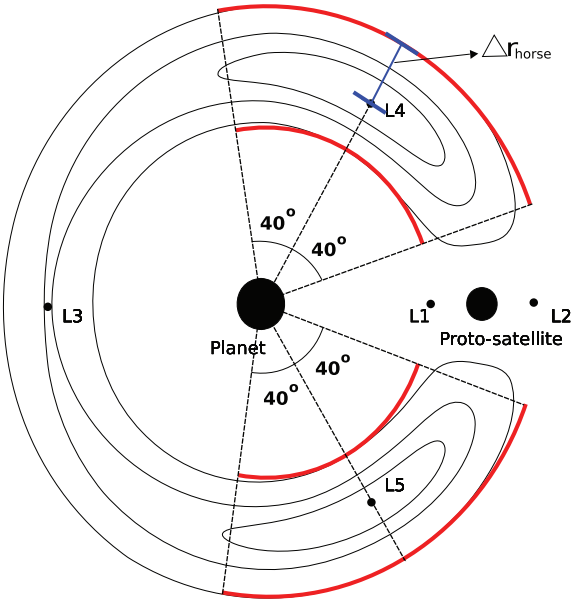

Figure 1. Schematic location of the sectors around L_4 and L_5 were the planetesimals are initially distributed. Each sector is delimited by an arc of 80°, centred on the Lagrangian point, and the extreme orbital radii of the largest horseshoe orbit. The half width of the largest horseshoe orbit, $\Delta r_{\rm horse}$, is given by equation (1).

The mass of the protosatelite might vary along the simulation due to some collisions with planetesimals, but its small growth do not affect significantly the dynamics of the planetesimals around the Lagrangian points (Fleming & Hamilton 2000).

The planetesimal clouds were always initially randomly distributed in a sector around L_4 or L_5. The sector is delimited by an arc of 80°, centred on the Lagrangian point, and the extreme orbital radii of the largest horseshoe orbit (Fig. 1). The half width of the largest horseshoe orbit is given by Dermott & Murray (1981a) as

$$\Delta r_{\rm horse} = \frac{1}{2}\mu_2^{1/3} a_2, \qquad (1)$$

where μ_2 and a_2 are the relative mass and the semimajor axis of the protosatellite, respectively. Studying the overlap of first-order mean motion resonances, Wisdom (1980) found an expression that gives the width of a chaotic region from the planar circular orbit of a secondary body. Therefore, it is important to have in mind that just outside the co-orbital region (interior and exterior) there is a chaotic region. Particles in this region usually tend to have close encounters with the protosatellite and get large eccentricities, leaving the neighbourhood. Since we are interested in the formation of the small counterparts of co-orbital satellite systems, in general, we considered clouds of planetesimals with the total mass of the order of the smaller co-orbital satellites, given in Table 1. We also considered that all planetesimals have the same initial mass, $m_{\rm p_i}$. We performed simulations for different clouds of planetesimals. We adopted clouds of 10^3, 5×10^3 and 10^4 planetesimals each one for three different values of $m_{\rm p_i}$, 10^{-12}, 10^{-13} and 10^{-14} masses of Saturn.

The simulations were made through numerical integrations using the Burlish–Stoer integrator from the package MERCURY (Chambers 1999). The length of the integration, τ (in orbital periods of the protosatellite), varied according to the value of $m_{\rm p_i}$. For $m_{\rm p_i} = 10^{-12}$ it was used $\tau = 10^5$, for $m_{\rm p_i} = 10^{-13}$ it was used $\tau = 10^6$ and for $m_{\rm p_i} = 10^{-14}$ it was used $\tau = 10^7$. That is necessary due to the gravitational attraction between the planetesimals, which is smaller as smaller are their masses, leading to a longer time for the system to evolve.

For each cloud of planetesimals with a specific value of $m_{\rm p_i}$ we performed at least two independent simulations. One placing it around L_4 and the other around L_5. We also tested the effect of Saturn's oblateness by running extra simulations with the inclusion of the J_2 term in the gravitational potential of the central body. The planetesimals in all simulations were initially placed in circular orbits.

3 NUMERICAL SIMULATIONS

Along the numerical simulations the planetesimals collide among them generating lager planetesimals. The collisions are always considered constructive, i.e. inelastic collisions. By the end of the integration time there are only a few (at most four) large planetesimals left. The final masses of the remaining planetesimals are represented by $m_{\rm p_f}$.

In order to have an idea of the time evolution of these systems we present a sample of snapshots for two representative simulations. Fig. 2 shows the dynamical evolution of a cloud of 10^4 planetesimals with $m_{\rm p_i} = 10^{-13}$, initially distributed around L_4. In each frame are shown the values of the osculating semimajor axis and eccentricities of the remaining planetesimals at a given moment. The orbital radius of the protosatellite is considered as unity. The colour grade indicates the mass of the planetesimal.

Since we are interested in the formation of small co-orbital satellites, the best candidates should be the remaining planetesimals with low eccentricity and semimajor axis inside the co-orbital region. So we included in the plots the dashed curves that indicate the co-orbital region defined by the largest horseshoe width ($1 \pm \Delta r_{\rm horse}$). In general, the planetesimals that leave the co-orbital region present chaotic behaviour and collide with the protosatellite.

From the plots of Fig. 2 we notice that the eccentricities of the planetesimals increase as they start to grow. However, they are limited to low values ($e < 0.007$). After about 1068 yr there are only three planetesimals left and it takes about a thousand years to reach a single planetesimal. That last one has a mass of $m_{\rm p_f} = 5.1170E - 10$.

In Fig. 3 we present the dynamical evolution of a cloud of 10^3 planetesimals with $m_{\rm p_i} = 10^{-14}$, initially distributed around L_5. The evolution is very much similar to that presented in Fig. 2. However, at least two major differences should be pointed out. The eccentricities do not get much larger then 0.001 and the time scales are much longer then in the previous case. These two features are naturally due to the lower values of the initial mass of the planetesimals, $m_{\rm p_i}$, and the total mass of the cloud of the planetesimals. Larger masses produce stronger gravitational interactions accelerating the evolution of the system and increasing the values of eccentricities.

The evolutions of all the other numerical simulations we have performed are similar to these ones. However, the plots presented in Figs 2 and 3 do not guarantee that the remaining planetesimals are in co-orbital orbits with the protosatellite. Therefore, we analysed the evolution of the angle θ between the remaining planetesimals and the protosatellite, called libration angle. This angle is defined as the difference in mean longitudes, $\theta = \lambda_{\rm p} - \lambda_2$, where $\lambda_{\rm p}$ and λ_2 are the mean longitudes of the planetesimal and secondary body, respectively. A representative sample of such evolution is presented in Figs 4–7. In each figure we present two plots. The top plot shows the evolution of θ and the bottom one shows the evolution the of planetesimal's mass. All plots cover the whole integration time and

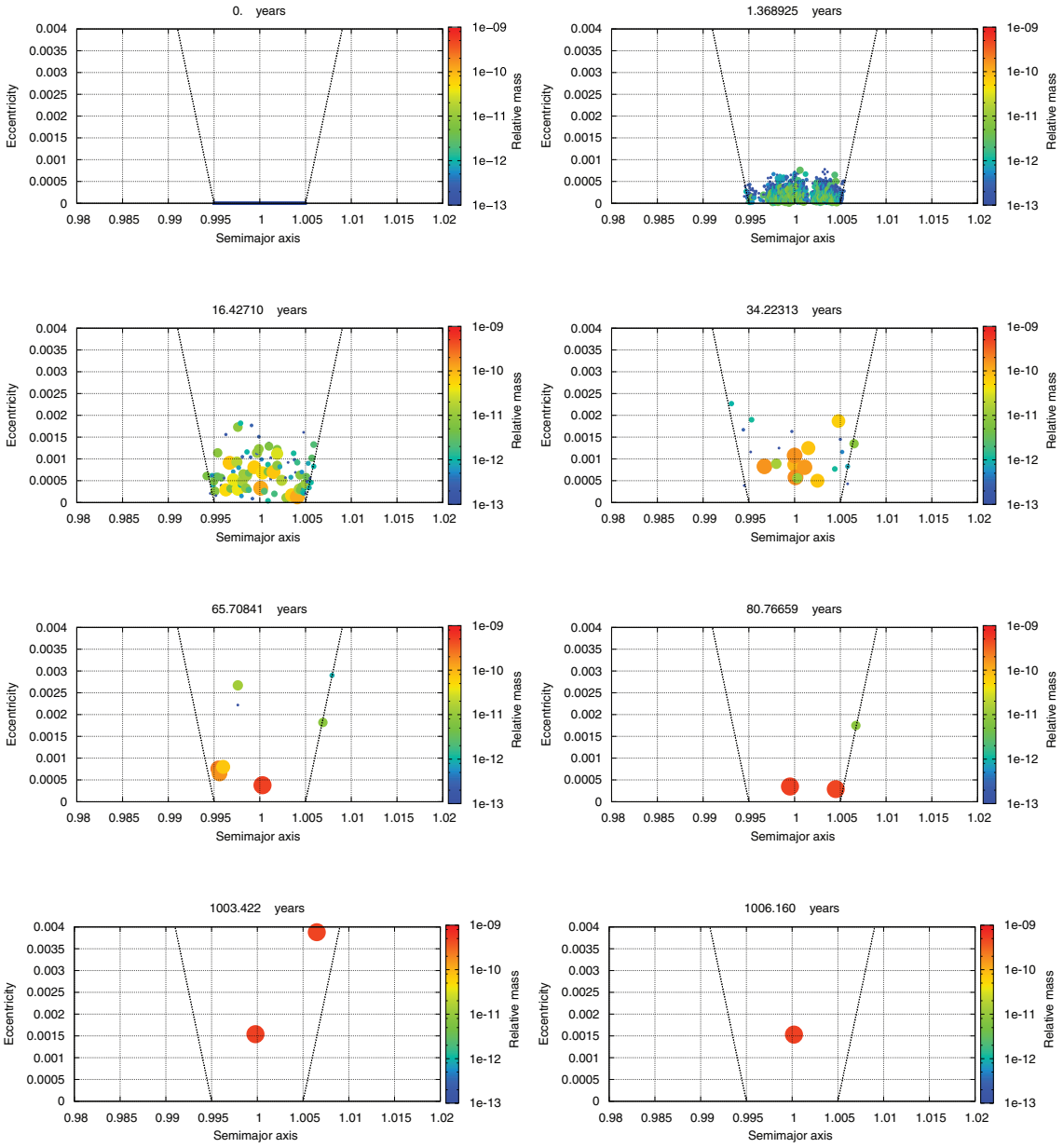

Figure 2. Dynamical evolution of a cloud of 10^4 planetesimals with $m_{\rm pi} = 10^{-13}$, initially distributed around L_4. In each frame are shown the values of the osculating semimajor axis and eccentricities of the remaining planetesimals at a given moment. The colour grade indicates the mass of the planetesimal. The dashed curves indicate the co-orbital region defined by the largest horseshoe width ($1 \pm \Delta r_{\rm horse}$).

they are shown in a logarithmic scale. The temporal evolution of the libration angle confirmed that in all simulations the remaining planetesimals are in co-orbital trajectories. The plots show a complete variety of evolutions. Planetesimals that started in tadpole orbits around L_4 or L_5 and ended in horseshoe orbits (Figs 5 and 6). Planetesimals that started in tadpole orbit around L_4 and ended in tadpole orbit around L_5 (Fig. 4) or in tadpole orbit around L_4 (Fig. 7). The evolutions are not always smooth. There are cases of tadpole orbits that 'jump' from L_4 to L_5 and then again back to L_4 (Fig. 7), and others that 'jump' from L_5 to L_4 and then to a horseshoe orbit (Fig. 6).

The changes in the amplitude of oscillation of the co-orbital planetesimals along their evolution are associated to the collisions with other planetesimals. Several of these changes can clearly be seen by comparison between the top and the bottom plots of each figure. For example, in Fig. 6 the last visible step in the growth of the planetesimal coincides with the change from tadpole to horseshoe orbit.

A summary of the whole set of simulations is presented in Tables 3 and 4. We performed 24 simulations neglecting the oblateness of Saturn (Table 3) and other 18 simulations taking it into account (Table 4). In the last two columns the kind of co-orbital trajectory and the final mass of the survivors planetesimals are shown. As we can see, in several simulations there were more then one planetesimal left. In some cases we followed the simulations for longer times. For example, simulation 13a (Table 3) was integrated for more than 10^5 yr and no extra collision occurred along the second half of such integration time. In the case of simulation 14a (Table 3), the integration was extended to 1 Myr and there were still two planetesimals left. One in horseshoe orbit and other in tadpole around L_5.

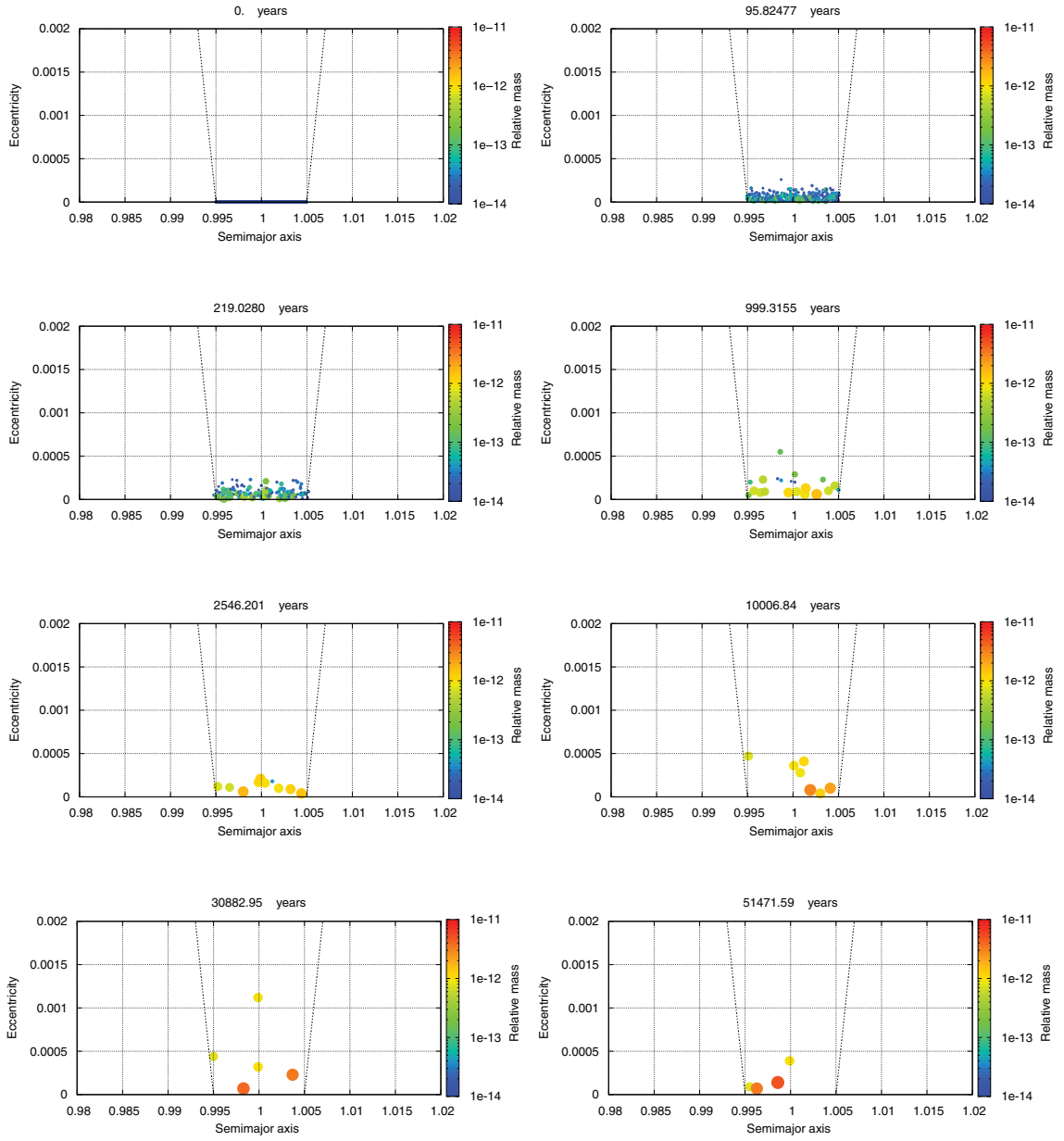

Figure 3. Dynamical evolution of a cloud of 10^3 planetesimals with $m_{\rm Pi} = 10^{-14}$, initially distributed around L_5. In each frame are shown the values of the osculating semimajor axis and eccentricities of the remaining planetesimals at a given moment. The colour grade indicates the mass of the planetesimal. The dashed curves indicate the co-orbital region defined by the largest horseshoe width ($1 \pm \Delta r_{\rm horse}$).

From Table 3 we have that 2/3 of the survivors are left in horseshoe trajectories, while the remaining 1/3 are equally divided in tadpole trajectories around L_4 and L_5. We also note that, in each simulation, the total mass of the survivors is very close to the corresponding total mass of initial cloud of planetesimals. The difference between these two values is the mass of planetesimals that collided with the protosatellite.

Comparing the simulations presented in Table 3 with those presented in Table 4, we can note that the oblateness of Saturn did not introduce any significant change in the results as a whole.

Beaugé et al. (2007) found that the final mass of the formed Trojans the kind of terrestrial planets did not depend significantly either on the initial mass or on the number of the initial population of planetesimals. In our simulations we do realize that the number of planetesimal and its initial mass play an important role in the final outcome.

In Table 3, we can see that the initial populations with small mass (10^{-13}, 10^{-14}) and small number of planetesimal (1000) have a larger tendency to yield more than one final body. This effect is caused by the weak gravitational attraction when the planetesimals are smaller and more distant from each other, consequently few collisions occur. However, when we have a lot of planetesimals, even with small mass, they are closer, then the gravitational attraction is larger and collisions become more frequent.

Although in most cases the final total mass is almost equal to the initial value, in one case there is a significant mass loss (Table 3, simulation 3). This occurred due to a collision of a larger planetesimal with the secondary body. However, for a similar

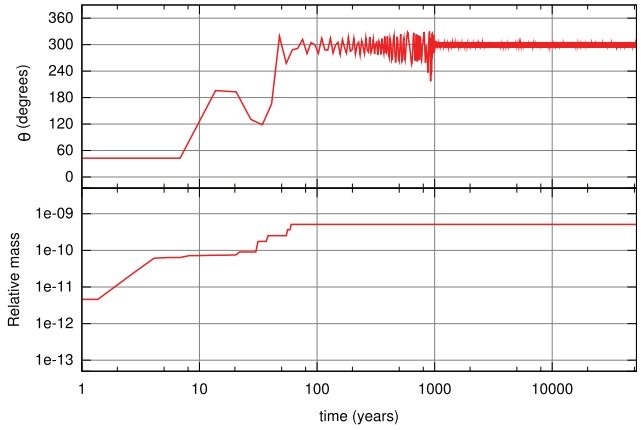

Figure 4. Temporal evolution of the libration angle (top) and the relative mass (bottom) of the remaining planetesimal from the simulation of a cloud of 10^4 planetesimals with $m_{\rm pi} = 10^{-13}$, initially distributed around L_4. After about 60 yr the planetesimal reaches its final mass, $m_{\rm pf} = 5.117 \times 10^{-10}$, and starts to librate around L_5.

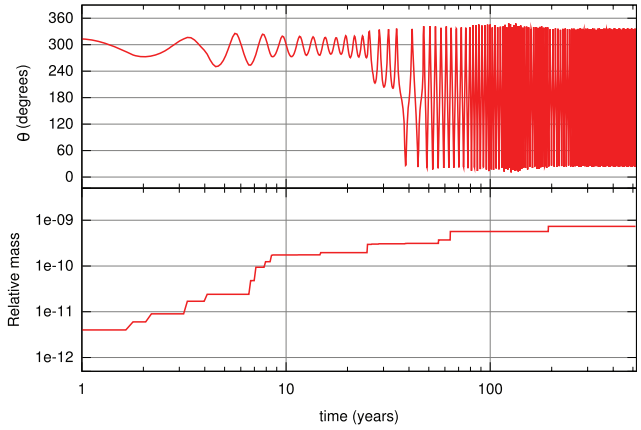

Figure 5. Temporal evolution of the libration angle (top) and the relative mass (bottom) of the remaining planetesimal from the simulation of a cloud of 10^3 planetesimals with $m_{\rm pi} = 10^{-12}$, initially distributed around L_5. By the end of the simulation the planetesimal reaches its final mass, $m_{\rm pf} = 7.35 \times 10^{-10}$, and stays in a horseshoe orbit.

initial planetesimal population distributed around L_5 there is no mass loss, this loss mass might be one statistical fluke, but this has to be checked with further studies.

The temporal evolution of the total number of the remaining planetesimals, N, in the system gives an idea of the different speeds at each stage of the system evolution. In Fig. 8 we present a representative sample of the temporal evolution of the total number of the remaining planetesimals of our simulations. In all the cases studied, the evolution of the system can be well represented by three stages. In the first stage there is a 'cold' cloud, the planetesimals are in near circular orbits and do not collide frequently. Then, along the time the gravitational interaction among the planetesimals 'heat' the cloud, the trajectories get some eccentricity and the rate of collisions increase, producing larger planetesimals. Larger planetesimals excite the cloud even more and also increase their sphere of influence, resulting in larger cross-sections and faster growing. When most of the planetesimals collided, there are a few left, then the collision rate decreases significantly and the evolution of the system slows down.

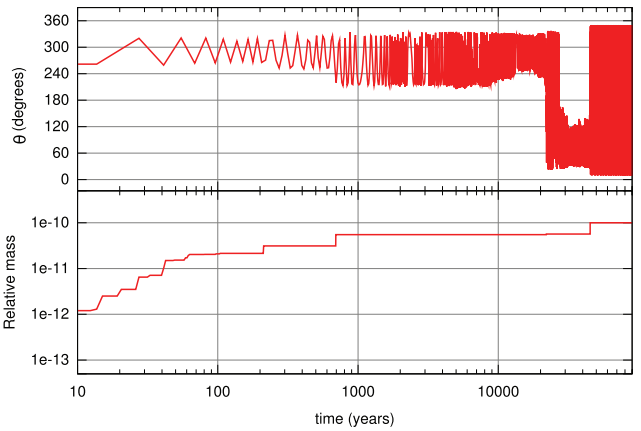

Figure 6. Temporal evolution of the libration angle (top) and the relative mass (bottom) of the remaining planetesimal from the simulation of a cloud of 10^3 planetesimals with $m_{\rm pi} = 10^{-13}$, initially distributed around L_4. By the end of the simulation the planetesimal reaches its final mass, $m_{\rm pf} = 10^{-10}$, and stays in a horseshoe orbit.

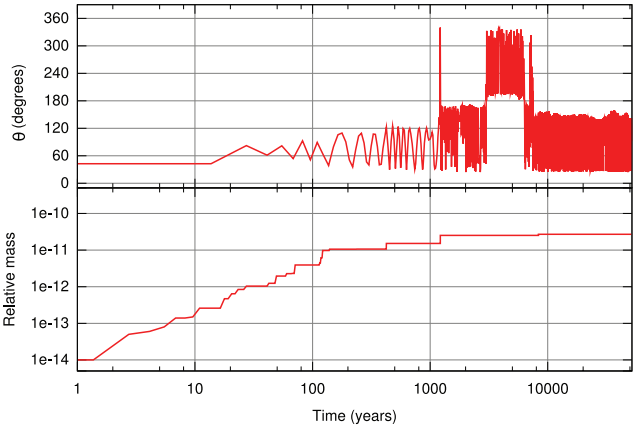

Figure 7. Temporal evolution of the libration angle (top) and the relative mass (bottom) of the remaining planetesimal from the simulation of a cloud of 5×10^3 planetesimals with $m_{\rm pi} = 10^{-14}$, initially distributed around L_4. After about 51 000 yr the planetesimal reaches its final mass, $m_{\rm pf} = 2.703 \times 10^{-11}$ and starts to librate in a tadpole orbit around L_4.

A comparison of the curves presented in Fig. 8 shows that the rate of decay of the total number of planetesimals is strongly dependent on the total mass of the initial cloud of planetesimals.

In order to infer possible effects due to mean motion resonances with nearby satellites on the mechanism of co-orbitals formation, we performed simulations considering Mimas and Thetys in 4:2 resonance of the type inclination. We considered a system composed of an oblate central body (Saturn), two satellites (Mimas–Thetys) which are in mean-motion resonance 4:2 and a cloud of planetesimals. The simulations were made for six cloud of 1000 planetesimal considering in each case $m_{\rm pi}$ equal to 10^{-12}, 10^{-13} or 10^{-14} around L_4 and L_5. It is important to have in mind that the previous simulations were in a planar system, and when we considered Mimas and Thetys in a 4:2 inclination-type resonance, the problem becomes three-dimensional. In general, these new simulations did not show any significant difference in comparison with the simulations presented in Table 4. In Fig. 9 we present a comparison of the temporal decaying number of the planetesimals for the simulations of a cloud of 10^3 planetesimals initially located around L_4 and with $m_{\rm pi} = 10^{-12}$. It shows that only in the final

Table 3. Set of simulations without Saturn's oblateness.

Simulation	Number of plantesimals	Location of initial distribution	Integration time (yr)	$m_{\rm pi}$	Trajectories of the survivors[a]	Final masses $m_{\rm pf}$
1	10 000	L_4	10 005	10^{-14}	H	10^{-10}
2	10 000	L_5	20 238	10^{-14}	H	10^{-10}
3	10 000	L_4	1068	10^{-13}	T_{L_5}	5.117×10^{-10}
4	10 000	L_5	99	10^{-13}	H	9.999×10^{-10}
5	10 000	L_4	51	10^{-12}	H	9.969×10^{-9}
6	10 000	L_5	50	10^{-12}	H	9.974×10^{-9}
7	5000	L_4	51 000	10^{-14}	H, T_{L_4}	2.297×10^{-11}, 2.703×10^{-11}
8	5000	L_5	51 000	10^{-14}	H, T_{L_5}	2.53×10^{-11}, 2.47×10^{-11}
9	5000	L_4	3325	10^{-13}	H	4.961×10^{-10}
10	5000	L_5	989	10^{-13}	H	4.943×10^{-10}
11	5000	L_4	52	10^{-12}	H	3.602×10^{-9}
12	5000	L_5	61	10^{-12}	T_{L_5}	3.369×10^{-9}
13a	1000	L_4	51 000	10^{-14}	H, H, T_{L_4}	3.45×10^{-12}, 1.94×10^{-12}, 4.61×10^{-12}
13b	1000	L_4	51 000	10^{-14}	T_{L_4}, H, H	2.54×10^{-12}, 2.21×10^{-12}, 5.25×10^{-12}
14a	1000	L_5	51 000	10^{-14}	H, T_{L_5}, H, H	3.35×10^{-12}, 9.6×10^{-13}, 4.92×10^{-12}, 7.7×10^{-13}
14b	1000	L_5	51 000	10^{-14}	H, H, H, T_{L_5}	1.51×10^{-12}, 5.03×10^{-12}, 2.14×10^{-12}, 1.33×10^{-12}
15a	1000	L_4	5100	10^{-13}	H, T_{L_4}	5.38×10^{-11}, 4.62×10^{-11}
15b	1000	L_4	5100	10^{-13}	T_{L_4}, H	4.24×10^{-11}, 5.76×10^{-11}
16a	1000	L_5	5100	10^{-13}	T_{L_4}, H, T_{L_5}	1.7×10^{-12}, 4.32×10^{-11}, 5.51×10^{-11}
16b	1000	L_5	5100	10^{-13}	H, T_{L_5}	4.28×10^{-11}, 5.72×10^{-11}
17a	1000	L_4	510	10^{-12}	T_{L_4}, H	6.99×10^{-10}, 2.52×10^{-10}
17b	1000	L_4	229	10^{-12}	H	9.32×10^{-10}
18a	1000	L_5	192	10^{-12}	H	7.35×10^{-10}
18b	1000	L_5	277	10^{-12}	H	10^{-9}

[a]Horseshoe (H), tadpole around L_4 (T_{L_4}) and tadpole around L_5 (T_{L_5}).

Table 4. Set of simulations with Saturn's oblateness.

Simulation	Number of plantesimals	Location of initial distribution	Integration time (yr)	$m_{\rm pi}$	Trajectories of the survivors[a]	Final masses $m_{\rm pf}$
1	10 000	L_4	51 000	10^{-14}	H, H	$1,612 \times 10^{-11}$, 8.388×10^{-11}
2	10 000	L_5	14 672	10^{-14}	H	10^{-10}
3	10 000	L_4	654	10^{-13}	H	8.666×10^{-10}
4	10 000	L_5	218	10^{-13}	H	9.822×10^{-10}
5	10 000	L_4	55	10^{-12}	H	9.382×10^{-9}
6	10 000	L_5	59	10^{-12}	H	9.923×10^{-9}
7	5000	L_4	51 000	10^{-14}	H, T_{L_4}	2.646×10^{-11}, 2.354×10^{-11}
8	5000	L_5	51 000	10^{-14}	H, T_{L_4}	2.119×10^{-11}, 2.881×10^{-11}
9	5000	L_4	2308	10^{-13}	H	4.926×10^{-10}
10	5000	L_5	1663	10^{-13}	H	5×10^{-10}
11	5000	L_4	95	10^{-12}	H	4.445×10^{-9}
12	5000	L_5	49	10^{-12}	H	4.333×10^{-9}
13	1000	L_4	51 000	10^{-14}	H, H, H, T_{L_4}	3.18×10^{-12}, 3.45×10^{-12}, 1.79×10^{-12}, 1.58×10^{-12}
14	1000	L_5	51 000	10^{-14}	H, H, T_{L_5}	4.39×10^{-12}, 2.12×10^{-11}, 3.49×10^{-11}
15	1000	L_4	29 768	10^{-13}	H	6.78×10^{-11}
16	1000	L_5	51 000	10^{-13}	T_{L_5}, H	4.37×10^{-11}, 5.63×10^{-11}
17	1000	L_4	218	10^{-12}	H	9.86×10^{-10}
18	1000	L_5	173	10^{-12}	H	9.99×10^{-10}

[a]Horseshoe (H), tadpole around L_4 (T_{L_4}) and tadpole around L_5 (T_{L_5}).

stages (after reducing the number of planetesimals to about 30 per cent) the results present some notable difference. The results under resonant perturbation evolve more slowly than the system without such perturbation. Probably, this is only due to the fact that the system under resonant perturbation is in a three-dimensional space, which reduces the chances of encounters between the planetesimals in comparison with the planar system case.

4 FINAL COMMENTS

In this work we present results of numerical simulations in order to study the viability of the congenital formation approach as a mechanism for the origin of the co-orbital satellites of Thetys and Dione. We considered that the collisions are always inelastic and make the growth of the planetesimals. The results show that almost

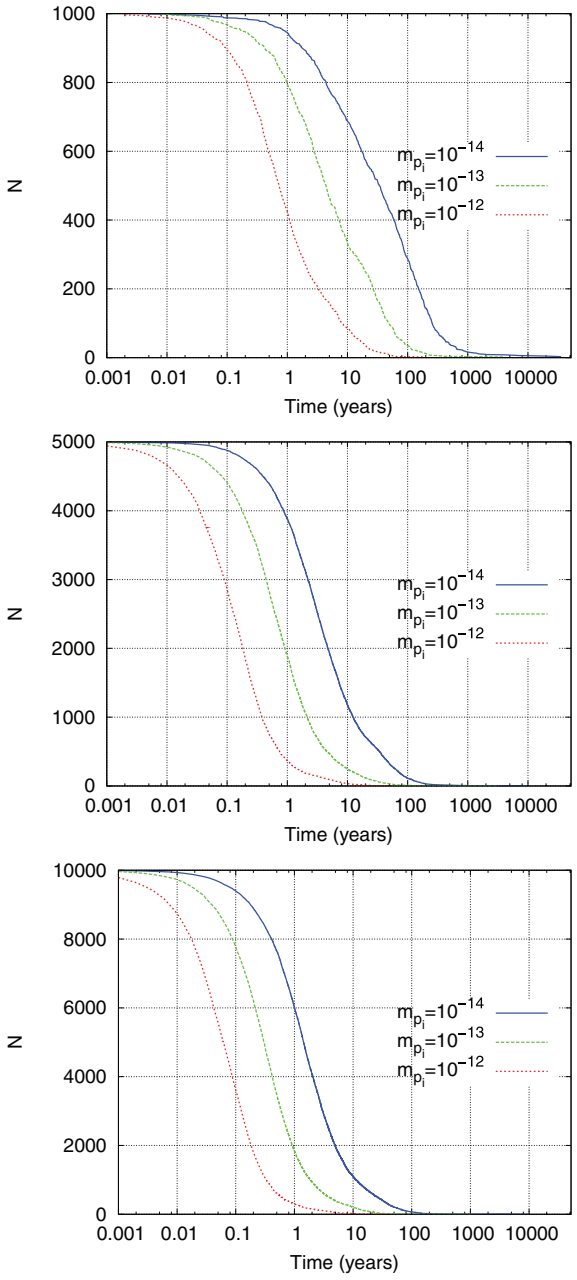

Figure 8. Temporal evolution of the total number of remaining planetesimals. It is shown the data from simulations of clouds of 10^3 (top), 5×10^3 (middle) and 10^4 (bottom) planetesimals around L_4 with initial masses $m_{p_i} = 10^{-14}$, 10^{-13} and 10^{-12}.

all the initial mass of the clouds are converted in one or a few planetesimals in co-orbital motion with the protosatellite. The final masses are of the same order of the small co-orbital satellites: Helene, Polydeuces, Telesto and Calypso. Therefore, we found that this is a promising mechanism for this purpose.

The distribution of librational amplitudes of the final bodies that remain in tadpole orbits varies from 4° up to 75°. The real co-orbitals have a libration amplitude of which varies from 1.3° up to 25.9°. However, some mechanisms could reduce the amplitude of libration, for example, the gas drag (Chanut et al. 2008), mass accretion or radial migration of the secondary body (Fleming & Hamilton 2000).

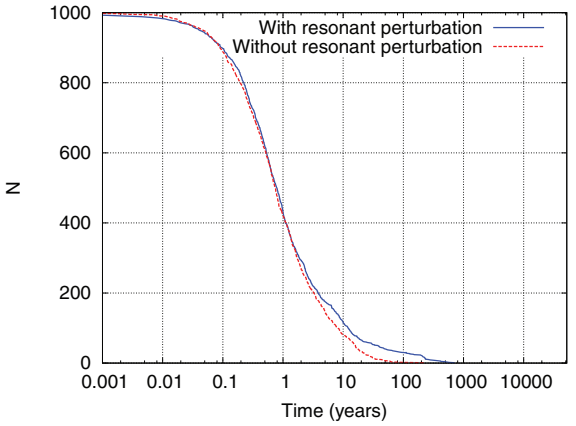

Figure 9. Temporal evolution of the total number of remaining planetesimals. It is shown the data from simulations of clouds of 10^3 with initial masses $m_{p_i} = 10^{-12}$ initially distributed around L_4. The red and dashed line correspond to a simulation only with Thetys and the blue and solid line correspond to a simulation with Thetys and Mimas in mean motion resonance 4:2.

In this paper we do not consider these mechanisms, but might be included in future works.

The effects of mean motion resonances of nearby satellites shows to be of no significative relevance for the present model of congenital formation of co-orbitals.

The results presented here might look like obvious. However, in Beaugé et al (2007) it was found that a growing planetary embryo generates a chaotic region around the Lagrangian point, inhibiting additional accretion and setting a limit in the final mass of the co-orbital body. They studied the possibility of congenital formation of Earth-like planets in co-orbital orbits of exoplanetary systems. In their work they adopted systems like the Jupiter–Sun system, with relative mass of 10^{-3}, and did not manage to form co-orbital planets with mass larger than 0.6 $M_\oplus$ This phenomena does not occur in the present work because the results of the simulation are strongly dependent on the relative mass of the secondary body (Izidoro, Winter & Tsuchida, in preparation).

It is important to comment that in the present congenital model the final co-orbitals formed are of similar masses. However, Dione has one co-orbital, Helene whose mass is about two orders of magnitude higher than the other co-orbital, Polydeuces. Therefore, the model as considered in the present work is not able to explain by itself alone such configuration. Consequently, there is still plenty of work to be done.

ACKNOWLEDGMENTS

The comments and questions of an anonymous referee helped to improve this paper. This work was supported by the Brazilian agencies CAPES and CNPq, and by the Foundation of the State of São Paulo FAPESP.

REFERENCES

Armitage P. J., 2007, preprint (astro-ph/0701485)
Beaugé C., Sándor Zs., Érdi B., Süli A., 2007, A&A, 463, 359
Chambers J., 1999, MNRAS, 304, 793
Chanut T., Winter O. C., Tsuchida M., 2008, A&A, 481, 519
Christou A. A., Namouni F., Morais M. H. M., 2007, Icarus, 192, 106
Connors M., 2005, Planet. Space Sci., 53, 617
Dermott S. F., Murray C. M., 1981a, Icarus, 48, 1

Dermott S. F., Murray C. M., 1981b, Icarus, 48, 12
Fleming J. H., Hamilton D. P., 2000, Icarus, 148, 479
Giorgini J. D. et al., 1996, BAAS, 28, 1158
Greenberg R., 1989, in Atreya S. K., Pollack J. B., Matthews M. S., eds, Origin and Evolution of Planetary and Satellite Atmosphere. Univ. Arizona Press, Tucson, p. 137
Hayashi C. K., Nakazawa K., Nakagawa Y., 1985, in Black D. C., Matthews M. S., eds, Protostar and Planets II. Univ. Arizona Press, Tucson, p. 1100
Innanen K. A., 1991, J. R. Astron. Soc. Canada, 85, 151
Jacobson R. A., 2004, BAAS, 36, 1097
Lecacheux J., Laques P., Vapillon L., Auge A., Despiau R., 1980, Icarus, 43, 111
Mourão D. M., Winter O. C., Tokoyama T., Cordeiro R. R., 2006, MNRAS, 372, 1614
Murray C. D., Cooper N. J., Evans M. W., Beurle K., 2005, Icarus, 179, 222
Porco C. C., Thomas P. C., Weiss J. W., Richardson D. C., 2005, Sci, 307, 1226
Reitsema H. J., 1981, Icarus, 48, 140
Reitsema H. J., Smith B. A., Larson S. M., 1980, Icarus, 43, 116
Safronov V. S., 1969, Evolution of the Protoplanetary Cloud and the Formation of the Earth and Planets. Nauka Press, Moscow. English translation: NASA TT F-677
Smith B. A., Voyager Imaging Team, 1981, Sci, 212, 504
Tabachnik S., Evans N. W., 1999, ApJ, 517, L63
Veillet C., 1981, A&A, 102, L5
Wetherill G. W., 1980, ARA&A, 18, 77
Wetherill G. W., 1990, Annu. Rev. Earth Planet. Sci., 18, 205
Wisdom J., 1980, AJ, 85, 1122
Yoder C. F., Colombo G., Synnott S. P., Yoder K. A., 1983, Icarus, 53, 431
Zhou L.-Y., Dvorak R., Sun Y., 2009, MNRAS, 398, 1217

This paper has been typeset from a TEX/LATEX file prepared by the author.